J. Fluid Mech. (1969), *vol.* 38, *part* 2, *pp.* 225–242
Printed in Great Britain

Some electrically driven flows in magnetohydrodynamics Part 3. The asymptotic theory for flow between circular electrodes

By J. C. R. HUNT
Central Electricity Research Laboratories, Leatherhead, Surrey
AND K. STEWARTSON
University College London

(Received 4 September 1968 and in revised form 12 March 1969)

In this, the third, part we present a complete asymptotic analysis of the distribution of velocity and electric potential in an electrically conducting liquid between two circular electrodes of finite diameter, $2b$, when a current is passed between them. The electrodes are set opposite to each other in insulating planes, a distance $2a$ apart, and a magnetic field is applied perpendicular to these planes.

The asymptotic solution is obtained under the restriction that the Hartmann number M satisfies both the conditions $M \gg 1$ and $M^{\frac{1}{2}}l \gg 1$, where $l = b/a$. It enables us to calculate the distribution of velocity and electrical potential throughout the flow field, and provides an expansion for the resistance R between the electrodes in descending powers of $M^{\frac{1}{2}}l$, which is correct provided terms of order M^{-1} and $(lM^{\frac{1}{2}})^{-3}$ are neglected. Comparison of the theoretical results with experiment shows good agreement in the measurements of R and in the direct probe measurements of electrical potential within the fluid. This is one of the first experiments in which direct probe measurements of an MHD flow, as well as external measurements, have provided such a satisfactory confirmation of the theory. Direct measurements of the velocity, by means of a Pitot tube as in part 2, or by means of a hot-film anemometer undertaken by Malcolm (1968), agree less well with the theory.

1. Introduction

In parts 1 and 2 of this paper Hunt & Williams (1968) and Hunt & Malcolm (1968) have examined some of the interesting fluid dynamic and electrical phenomena which occur when a current is passed through an electrically conducting fluid placed between two planes which contain various kinds of electrode, and a magnetic field is imposed perpendicular to the planes (see figure 1). The physical effects that occur are caused by the tendency of the current lines to bulge out from the region between the electrodes so as to produce an electromagnetic $\mathbf{j} \times \mathbf{B}$ force on the fluid. In the case of circular electrodes, as explained in part 2, the final outcome of the various processes involved is that in narrow layers joining the rims of the electrodes an intense circumferential jet is created and the current

lines are confined to the cylinder joining the electrodes. In part 1 the effects of line and point electrodes were examined theoretically and in part 2 the analysis was extended to include the effects of circular electrodes which are perfectly conducting and have finite radius.

Hunt & Malcolm did not obtain a complete solution to the analytical problem, but were able to draw some conclusions of physical interest by means of an approximate asymptotic analysis when the Hartmann number $M \gg 1$. Some experiments were then described in which direct measurements of velocity and electric potential were made in the fluid. The experiments were difficult to perform, and liable to many errors, the art of measuring magnetohydrodynamic flows being in such a primitive state. However, some of the measurements were sufficiently repeatable and reliable and the Hartmann numbers were sufficiently high ($M > 600$) that the conclusions of the theory could be tested. Since the experimental results broadly agreed with these conclusions, a complete asymptotic analysis to produce actual values of the velocity potential, which could be compared with the experimental values, seemed worth while. Since the experiments of Hunt & Malcolm, Malcolm (1968) has made further and more detailed measurements of velocity using a new method, namely a specially adapted hot-film anemometer. With these further measurements a reliable theory is all the more necessary to compare the various experimental methods.

Using the equations and the basic assumptions of Hunt & Malcolm, a thorough asymptotic analysis is presented in §§ 3–4 of this paper. A central feature of this analysis is the solution of the singular integral equation (3.28) which leads to the result that an intense current sheet emanates from an annulus of thickness of $O(\mathrm{M}^{-1})$ at the electrodes' edges, a surprising fact since the thickness of the shear layers is $O(M^{-\frac{1}{2}})$. This phenomenon is analyzed in some detail in § 4. For comparison with the theory at $M \gg 1$, we present in § 3 an expression for the resistance when $M = 0$, and numerical results for the velocity and electric potential. In § 5 we compare the results of the theory with the experimental results of Hunt & Malcolm (1968) and Malcolm (1968) and find satisfactory agreement with the results of electric potential measurements but less satisfactory agreement with the results of direct measurements of velocity by Pitot tube and hot-film anemometer. Such discrepancies as cannot be explained by limitations of the experimental methods may be caused by the finite conductivity of the electrodes, which our analysis of § 3 does not account for.

2. Equations and boundary conditions

We consider an incompressible fluid, of conductivity σ and viscosity η, occupying the region between two parallel planes whose equations are $z = \pm a$ with respect to a set of cylindrical polar co-ordinates (r, θ, z) (see figure 1). Electrodes are inset flush with each plane extending over the disks $r \leqslant b$, while the remainder of each plane is assumed to be non-conducting, and a uniform magnetic field of flux density B_0 is applied in a direction perpendicular to them. A current I flows from one electrode to the other through the fluid, stimulating it into motion. The equations of magnetohydrodynamics governing the velocity v of the fluid

and the induced magnetic field h may, following Hunt & Williams (1968), be written:

$$0 = M\frac{\partial h}{\partial \zeta} + D_\rho(\rho v) + \frac{\partial^2 v}{\partial \zeta^2}, \tag{2.1}$$

$$0 = M\frac{\partial v}{\partial \zeta} + D_\rho(\rho h) + \frac{\partial^2 h}{\partial \zeta^2}, \tag{2.2}$$

$$-\frac{\partial h}{\partial \zeta} = -\frac{\partial \Phi}{\partial \rho} + Mv, \quad \frac{\partial h}{\partial \rho} + \frac{h}{\rho} = -\frac{\partial \Phi}{\partial \zeta}, \tag{2.3}$$

where

$$D_\rho = \frac{\partial}{\partial \rho}\left(\frac{1}{\rho}\frac{\partial}{\partial \rho}\right), \quad v = \frac{v_\theta}{I/2\pi a\sqrt{(\sigma\eta)}}, \quad h = \frac{h_\theta}{I/2\pi a}, \quad \Phi = \frac{\phi}{I/2\pi a\sigma},$$

$$\rho = \frac{r}{a}, \quad \zeta = \frac{z}{a}, \quad l = \frac{b}{a}, \quad \text{and} \quad M = B_0 a(\sigma/\eta)^{\frac{1}{2}}.$$

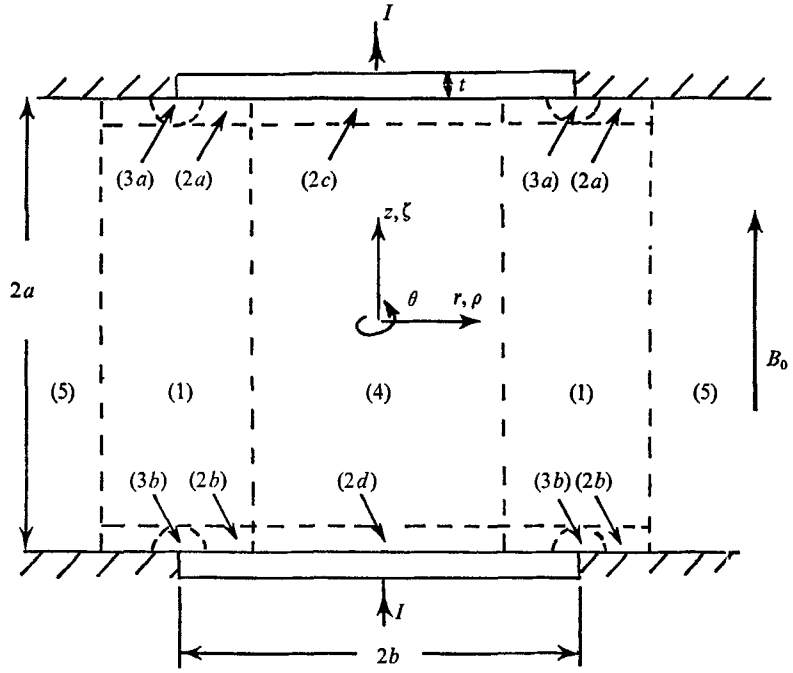

FIGURE 1. Diagram showing the position of the electrodes, the co-ordinate axes and the various regions used in the asymptotic analysis of § 3.

In equations (2.1) and (2.2) we have assumed that radial and axial velocities are zero, so that the only components of velocity are azimuthal and the only components of current density are radial and axial. It was shown by Hunt & Malcolm (1968, p. 799) that this condition is satisfied in practice if $M \gg 1$ and the current I is sufficiently small. Adding (2.1) and (2.2) we obtain the familiar combined equation in $(v+h)$:

$$\frac{M}{\rho}\frac{\partial}{\partial \zeta}[\rho(v+h)] + \left(\frac{1}{\rho}\frac{\partial^2}{\partial \zeta^2} + D_\rho\right)[\rho(v+h)] = 0. \tag{2.4}$$

Boundary conditions

The boundary conditions on the velocity v are simply

$$v = 0 \quad \text{at} \quad \zeta = \pm 1. \tag{2.5}$$

The boundary conditions on h, however, are more complicated and necessitate first considering the current distribution in the electrodes. Let the current distribution on the *outside* faces of the electrodes be

$$h = f_1(\rho) \quad \text{at} \quad \zeta = \pm(1+\tau), \tag{2.6}$$

where $t = a\tau$ is the electrode thickness. Since $\mathbf{j}$ the current density, at $\zeta = 1+\tau$, is bounded

$$f_1(0) = 0.$$

The total current entering and leaving the electrodes is

$$I = \int_0^b 2\pi r j_z \, dr$$

$$= \int_0^b 2\pi r \frac{1}{r}\frac{\partial}{\partial r}(rh_0)\, dr = Ilf_1(l).$$

Setting $$h = f_2(\rho) \quad \text{at} \quad \zeta = \pm 1, \tag{2.7}$$

it then follows that $$f_2(\rho) = \rho^{-1} \quad \text{when} \quad \rho = l, \tag{2.8}$$

since no current leaves the electrodes *via* their side walls.

We can now discuss the boundary conditions on h at $\zeta = \pm 1$ in the fluid and note first of all that the value of h in the containing walls and the fluid are the same at $\zeta = \pm 1$, so that (2.7) and (2.8) apply equally to h in the fluid. Now $f_2(\rho)$ can be directly calculated when $\rho > l$, for outside the electrodes the walls at $\zeta = \pm 1$ are insulating and therefore $j_z = 0$. It follows that $\partial\Phi/\partial\zeta = 0$ and hence, from (2.3),

$$h = f_2(\rho) = \frac{1}{\rho} \quad \text{at} \quad \zeta = \pm 1, \quad \rho > l, \tag{2.9}$$

there being no extra current source at $\rho = l$. If $\rho < l$, h is not known, but, from the condition that the radial component of electric field is the same in the fluid as in the electrode and (2.5), we have the condition

$$\left(\frac{\partial h}{\partial \zeta}\right)_f = \frac{\sigma}{\sigma_e}\left(\frac{\partial h}{\partial \zeta}\right)_e \quad \text{at} \quad \zeta = \pm 1, \quad \rho < l, \tag{2.10}$$

where f and e refer to the fluid and electrode, respectively.

It is now theoretically possible to calculate for any value of σ_e the distribution of current and velocity between the electrodes, given I and $f_1(\rho)$, using equations (2.1), (2.2) and (2.5) to (2.10). However, we are mainly interested in using these equations and boundary conditions to analyze the flow in the simplest case where the electrodes are highly conducting. Fortunately this case corresponds closely to the experimental situation and has the additional advantage that v and h are independent of $f_1(\rho)$. Thus for the remainder of this paper we shall replace (2.10) by

$$\partial h/\partial\zeta = 0 \quad \text{at} \quad \zeta = \pm 1, \quad \rho < l. \tag{2.11}$$

3. Asymptotic solution as $M \to \infty$

In this section we shall determine the principal features of the distribution of **v** and **h** between the electrodes, under the assumptions that

$$(a)\ M \gg 1, \quad (b)\ M^{\frac{1}{2}}l \gg 1, \quad \text{and} \quad (c)\ \sigma_e \tau/\sigma \to \infty. \tag{3.1}$$

The significance of the first of these conditions is that any primary (or Hartmann) boundary layers on the walls at $\zeta = \pm 1$ are thin compared with their distance apart, of the second that the thickness of the shear layers joining the rims of the electrodes must be small compared with their radii and of the third that the ratio of the conductivity of the electrodes to the fluid is very large. In general the conditions of any experiment will approximate to some of the criteria of (3.1) better than others; in the experiments of Hunt & Malcolm, $M \geqslant 175$, $\tau\sigma_e/\sigma > 7$ and $M^{\frac{1}{2}}l \geqslant 6$, since l is smaller than unity. In the asymptotic analysis below we only consider expansions of v and h in descending powers of $M^{\frac{1}{2}}l$, calculating a number of the leading terms for the various regions of the flow. The effect of a finite value of $\tau\sigma_e/\sigma$ has been considered in a separate investigation and was found to be of little significance.

Region (4)

We begin the analysis by discussing region (4) of figure 1, i.e. the region where $0 < \rho < l$, $|\zeta| < 1$, although as usual in core flow studies regions (2*c*) and (2*d*) play a vital role in controlling the solution in region (4). In region (4)

$$\frac{\partial}{\partial \rho} \sim \frac{1}{\rho}, \quad \frac{\partial}{\partial \zeta} \sim 1 \tag{3.2}$$

from the size of the region and hence to a first approximation (2.1) and (2.2) reduce to

$$h = f_2(\rho), \quad v = f_3(\rho), \tag{3.3}$$

terms of relative order M^{-1} being neglected. Now it follows from the boundary conditions and governing equations of § 2 that h is an even function of ζ while v is an odd function of ζ, so that

$$f_3(\rho) \equiv 0. \tag{3.4}$$

Hence on substituting (3.3), (3.4) back into (2.1), (2.2) and retaining terms $O(M^{-1})$ we find that

$$v = -(\zeta/M)\, D_\rho(\rho f_2) + O(M^{-2}), \quad h = f_2(\rho) + O(M^{-2}). \tag{3.5}$$

This solution while satisfying (3.1) does not satisfy the condition $v = 0$ at $\zeta = \pm 1$. We now consider the possibility that boundary layers in regions (2*c*) and (2*d*) can adjust v so that these conditions are satisfied. In such boundary layers $\partial/\partial\zeta \gg 1$ and (2.4) then has an additional complementary function of the form

$$A(\rho)\, e^{-M\zeta}. \tag{3.6}$$

It immediately follows that a boundary layer in $(v+h)$ can only exist near $\zeta = -1$, so that

$$v + h = f_2(\rho) - (\zeta/M)\, D_\rho(\rho f_2) + O(M^{-2}), \tag{3.7}$$

except near $\zeta = -1$, where

$$v+h = f_2(\rho)+(1/M)\,D_\rho(\rho f_2)+(1/M)\,A_+ e^{-M(\zeta+1)}+O(M^{-2}), \tag{3.8}$$

and A_+ is a function of ρ to be found and is independent of M. Similarly

$$v-h = -f_2(\rho)-(\zeta/M)\,D_\rho(\rho f_2)+O(M^{-2}), \tag{3.9}$$

except near $\zeta = 1$, where

$$v-h = -f_2(\rho)+(1/M)\,D_\rho(\rho f_2)+(1/M)\,A_- e^{+M(\zeta-1)}+O(M^{-2}), \tag{3.10}$$

and A_- is a function of ρ to be found. Combining (3.8), (3.9) it follows that the boundary conditions on v, h at $\zeta = -1$, namely (2.5) and (2.11), are satisfied if

$$A_+ = D_\rho(\rho f_2) = 0. \tag{3.11}$$

Hence

$$f_2(\rho) = \lambda\rho/l^2, \tag{3.12}$$

where λ is a constant to be found. Note that these results may be generalized to include the effect of a finite conductivity, σ_e, in the electrodes. The argument is omitted but we conclude that (3.11) is replaced by

$$D_\rho(\rho f_2) = \frac{\sigma}{\sigma_e \tau}(f_2 - f_1(\rho)), \tag{3.13}$$

whence $f_2(\rho)$ may be calculated in terms of $f_1(\rho)$. As already noted its effect is not important in the experiments.

The electric potential, $\Phi_{(4)}$, may now be calculated using (2.3), (3.3) and (3.12) to give

$$\Phi_{(4)} = -\frac{2\lambda\rho}{l^2}+O(M^{-1}). \tag{3.14}$$

Region (5)

Turning now to region (5) ($\rho > 1$, $|\zeta| < 1$) a similar line of argument can be adopted to that for region (4) except that now the boundary condition on h is that

$$h = 1/\rho, \quad \zeta = \pm 1, \quad \rho > l. \tag{3.15}$$

Hence (3.7) gives

$$1/\rho = f_2(\rho)-(1/M)\,D_\rho(\rho f_2)+O(M^{-2})$$

at $\zeta = 1$, so that in region (5)

$$f_2(\rho) = \frac{1}{\rho}, \quad v \equiv 0, \quad h \equiv \frac{1}{\rho}, \tag{3.16}$$

whence $\Phi \equiv 0$, the relative errors being at most $O(M^{-1})$.

Region (1)

There remains the discussion of region (1) together with its associated boundary layers on the planes of the electrodes. As things stand at the moment both h and Φ are discontinuous as $\rho \to l\pm$ in the limit $M \to \infty$ but we can make h continuous if we assume that $\lambda \to 1$. After examining various possibilities it appeared to us that a shear layer cannot be found to smooth out the discontinuity in h when M

is large unless $\lambda \to 1$ as $M \to \infty$. We therefore make this assumption and we shall find it leads to a consistent description of the flow field. We shall write, in fact,

$$\lambda = 1 + \frac{\lambda_1}{lM^{\frac{1}{2}}} + \frac{\lambda_2}{(lM^{\frac{1}{2}})^2} + O(M^{-1}, (lM^{\frac{1}{2}})^{-3}), \tag{3.17}$$

where λ_1, λ_2 are constants and then show that λ_1, λ_2 are $O(1)$. Thus we assume that when $M \gg 1$ the changes in h are small across region (1). Since λ is $O(1)$ the results (3.14) and (3.16) imply that the change in Φ across region (1) is $O(1)$.

The following change of variables is now introduced. Define

$$\begin{aligned} h &= \frac{1}{\rho} + \left(\frac{l}{\rho}\right)^{\frac{1}{2}} \hat{h}(\hat{\rho}, \zeta), \quad f_2(\rho) = \frac{1}{\rho} + \left(\frac{l}{\rho}\right)^{\frac{1}{2}} g(\hat{\rho}), \\ v &= \left(\frac{l}{\rho}\right)^{\frac{1}{2}} \hat{v}(\hat{\rho}, \zeta), \quad \hat{\rho} = \tfrac{1}{2}(l-\rho) M^{\frac{1}{2}}, \end{aligned} \tag{3.18}$$

where $g(\hat{\rho})$ is a function to be found and we have anticipated that the scale in the ρ direction is $O(M^{-\frac{1}{2}})$. In terms of $\hat{\rho}, \zeta$ the equations satisfied by $\hat{h}$, $\hat{v}$ are

$$\begin{aligned} \frac{\partial \hat{h}}{\partial \zeta} + \frac{1}{4}\frac{\partial^2 \hat{v}}{\partial \hat{\rho}^2} &= -\frac{1}{M}\frac{\partial^2 \hat{h}}{\partial \zeta^2} + \frac{3}{4}\frac{\hat{v}}{\rho^2 M}, \\ \frac{\partial \hat{v}}{\partial \zeta} + \frac{1}{4}\frac{\partial^2 \hat{h}}{\partial \hat{\rho}^2} &= -\frac{1}{M}\frac{\partial^2 \hat{v}}{\partial \zeta^2} + \frac{3}{4}\frac{\hat{h}}{M\rho^2}, \end{aligned} \tag{3.19}$$

and the corresponding boundary conditions are

$$\hat{v} = \partial \hat{h}/\partial \zeta = 0, \quad \hat{h} = g(\hat{\rho}) \qquad \text{at} \quad \zeta = \pm 1, \quad \hat{\rho} > 0, \tag{3.20a}$$

$$\hat{v} = \hat{h} = 0 \qquad \text{at} \quad \zeta = \pm 1, \quad \hat{\rho} < 0, \tag{3.20b}$$

$$\hat{v} \to 0, \quad \hat{h} \to 0 \qquad \text{as} \quad \hat{\rho} \to -\infty, \tag{3.20c}$$

$$\hat{v} \to 0, \quad \hat{h} - \frac{1}{l}\left[\frac{\rho}{l}\right]^{\frac{1}{2}}\left[\frac{\rho}{l}\lambda - \frac{l}{\rho}\right] \to 0 \qquad \text{as} \quad \hat{\rho} \to +\infty. \tag{3.20d}$$

So far no approximations have been made in deriving (3.19) and (3.20) except for the two limits $\hat{\rho} \to \pm\infty$ but now we assume that the terms on the right-hand side of (3.19) may be neglected—i.e. we ignore terms of relative order M^{-1} and $M^{-1}l^{-2}$. This assumption is valid over the region $\hat{\rho} = O(1)$, $|\zeta| < 1$, and then (3.19) leads to a single equation for $\hat{v} + \hat{h}$, namely

$$\left(\frac{\partial^2}{\partial \hat{\rho}^2} + 4\frac{\partial}{\partial \zeta}\right)(\hat{v} + \hat{h}) = 0, \tag{3.21}$$

with the solution

$$\hat{v} + \hat{h} = \frac{1}{\sqrt{[\pi(1-\zeta)]}} \int_{-\infty}^{\infty} G_1(t) \exp\left\{-\frac{(t-\hat{\rho})^2}{1-\zeta}\right\} dt, \tag{3.22}$$

where $G_1(t)$ is the limiting value of $\hat{v} + \hat{h}$ in region 1 as $\zeta \to 1$. Near $\zeta = 1$ boundary layers in $\hat{v}$ and $\hat{h}$ can occur to adjust the values of $\hat{v}$ and $\hat{h}$ as $\zeta \to 1$ in region (1) to the correct boundary conditions at $\zeta = 1$. However, no boundary layer is possible in $\hat{v} + \hat{h}$, for the same reason as in (3.6), and hence

$$G_1(\hat{\rho}) = 0, \quad \hat{\rho} < 0; \quad G_1(\hat{\rho}) = g(\hat{\rho}), \quad \hat{\rho} > 0. \tag{3.23}$$

A boundary layer is possible, however, near $\zeta = -1$ and analogously to (3.8) we then have

$$\hat{v}+\hat{h} = G_2(\hat{\rho}) + B_+(\hat{\rho})\, e^{-M(\zeta+1)}, \tag{3.24}$$

where $B_+(\hat{\rho})$ is a function of $\hat{\rho}$ to be found while $G_2(\hat{\rho})$ is the limit of $\hat{v}+\hat{h}$ as $\zeta \to -1$ according to (3.22).

From (3.20)

$$B_+(\hat{\rho}) = -G_2(\hat{\rho}) \quad \text{if} \quad \hat{\rho} < 0, \tag{3.25}$$

while

$$g(\hat{\rho}) = G_2(\hat{\rho}) + B_+(\hat{\rho}) \quad \text{if} \quad \hat{\rho} > 0. \tag{3.26}$$

On the other hand an analogous argument to (3.11) shows that if $\hat{\rho} > 0$

$$B_+(\hat{\rho}) = 0 \quad \text{and hence} \quad g(\hat{\rho}) = G_2(\hat{\rho}). \tag{3.27}$$

It then follows from (3.22), (3.23) and (3.27) that $g(\hat{\rho})$ satisfies the integral equation

$$g(\hat{\rho}) = \frac{1}{\sqrt{(2\pi)}} \int_0^\infty g(t) \exp\{-\tfrac{1}{2}(t-\hat{\rho})^2\}\, dt. \tag{3.28}$$

Further, to obtain the boundary condition on $g(\hat{\rho})$ as $\hat{\rho} \to \infty$, we use the fact that $g(\hat{\rho}) = h$ at $\zeta = \pm 1$. Then (3.20*d*) and (3.17) show that as $\hat{\rho} \to \infty$

$$g(\hat{\rho}) = -\frac{1}{l^2 M^{\frac{1}{2}}}\left[4 + \frac{3\lambda_1}{lM^{\frac{1}{2}}}\right]\left[\hat{\rho} - \frac{\lambda_1}{4} - \frac{4\lambda_2 - 3\lambda_1^2}{16 l M^{\frac{1}{2}}} + O(M^{-1}, (lM^{\frac{1}{2}})^{-3})\right]. \tag{3.29}$$

If we now write

$$g(\hat{\rho}) = -\frac{1}{l^2 M^{\frac{1}{2}}}\left[4 + \frac{3\lambda_1}{lM^{\frac{1}{2}}}\right]\hat{g}(\hat{\rho}), \tag{3.30}$$

then $\hat{g}(\hat{\rho})$ also satisfies the homogeneous integral equation (3.28). The boundary condition becomes

$$\text{as} \quad \hat{\rho} \to \infty, \quad \hat{g}(\hat{\rho}) - \hat{\rho} \to \text{const.}, \tag{3.31}$$

where the constant is unknown.

Since we have no information, as yet, about region (3) there is no boundary condition on $\hat{g}(\hat{\rho})$ as $\hat{\rho} \to 0$. However, Stewartson (1968) found that the condition (3.31) completely specifies the solution to (3.28), which, in turn, determines the constant in (3.31). He found the asymptotic series for $\hat{g}(\hat{\rho})$ to be

$$\text{as} \quad \hat{\rho} \to 0, \quad \hat{g}(\hat{\rho}) \sim \frac{1}{\sqrt{2}}\left[1 + \frac{\hat{\rho}\zeta(\frac{3}{2})}{\sqrt{(2\pi)}} + \frac{\hat{\rho}^2\zeta^2(\frac{3}{2})}{8\pi} + \frac{\hat{\rho}^3}{6\sqrt{2}\,\pi}\left\{\frac{\zeta^3(\frac{3}{2})}{12\pi} - \zeta(\tfrac{5}{2})\right\} + \ldots\right], \tag{3.32}$$

$$\text{as} \quad \hat{\rho} \to \infty, \quad \hat{g}(\hat{\rho}) - \hat{\rho} \to \frac{\zeta(\frac{1}{2})}{\sqrt{(2\pi)}}, \tag{3.33}$$

where

$$\zeta(s) = \sum_{n=1}^{\infty} n^{-s}.$$

Thus the constant in (3.31) is $\zeta(\frac{1}{2})/\sqrt{(2\pi)}$, whence

$$\lambda_1 = \frac{4\zeta(\frac{1}{2})}{\sqrt{(2\pi)}} = -2{\cdot}3304 \quad \text{and} \quad 4\lambda_2 = 3\lambda_1^2. \tag{3.34}$$

Using the numerical data of Hammersley (1961), who solved a similar integral equation, $\hat{g}(\hat{\rho})$ was calculated numerically and was found to agree with Stewartson's (1968) asymptotic formulae.

From (3.32) we immediately deduce that, whereas $f_2(\rho) = 1/l$ when $\rho = l$,

$$f_2(\rho) \to \frac{1}{l} - \frac{2\sqrt{2}}{l^2 M^{\frac{1}{2}}} + \ldots \quad \text{as} \quad (l-\rho)\, M^{\frac{1}{2}} \to 0+. \tag{3.35}$$

This jump in $f_2(\rho)$ near $\rho = l$ of $2\sqrt{2}/l^2 M^{\frac{1}{2}}$ shows that a quantity of current $O(M^{-\frac{1}{2}}I)$ emanates from the narrow region (3) on the electrode, i.e. the same quantity of current (to an order of magnitude) that emanates from region (2). Since the width of region (3) is $O(M^{-1})$ it follows that the current *density*, j_z, and electric field $\partial\phi/\partial z$ are $O(M^{\frac{1}{2}})$. In the light of this result, namely that the change of $f_2(\rho)$ in region (3) is of the same order as that in region (2), it seems especially remarkable that $f_2(\rho)$ in region (2) is only a function of regions (1) and (4). These surprising changes in $f_2(\rho)$ in regions (2) and (3) are illustrated schematically in figure 2.

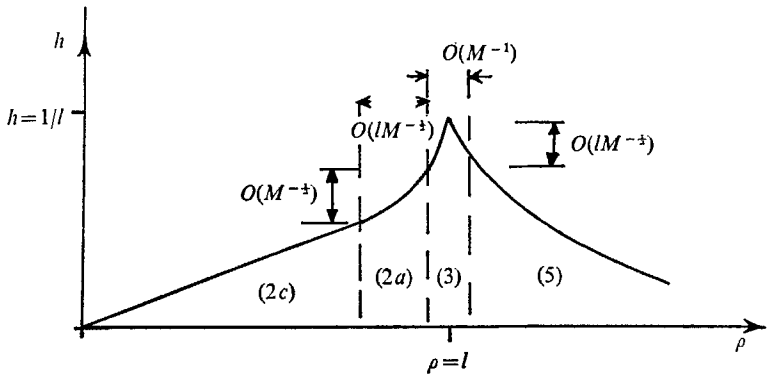

FIGURE 2. A schematic graph of $h(\rho)$ at $\zeta = \pm 1$, showing the regions (2*a*) and (3) in which the integral equation of § 3 and the Wiener–Hopf problem of § 4, respectively, have to be solved.

The resistance R may now be calculated, where R is defined by

$$R = \frac{2\Delta\phi}{I} = \frac{\Delta\Phi}{2\pi a\sigma}, \tag{3.36}$$

and $\mp\Delta\phi = \mp\Delta\Phi[I/(2\pi a\sigma)]$ is the potential at $\zeta = \pm 1$. To calculate Φ in region (4) we use (3.14) and (3.17):

$$\Phi_{(4)} = -\frac{2\zeta}{l^2}\left[1 + \frac{\lambda_1}{lM^{\frac{1}{2}}} + \frac{\lambda_2}{l^2 M} + \ldots\right], \tag{3.37}$$

so that the resistance is

$$R = \frac{2a\lambda}{\pi\sigma b^2} = R_\infty\left[1 - \frac{2{\cdot}330}{lM^{\frac{1}{2}}} + \frac{4{\cdot}073}{(lM^{\frac{1}{2}})^2} + \ldots\right], \tag{3.38}$$

where $R_\infty = 2a/\pi\sigma b^2$ is the electrical resistance of a cylinder of fluid, length $2a$ and radius b. We note that the first term in the asymptotic expansion of (3.38) about $M = \infty$ was obtained by Hunt & Malcolm (1968) and is independent of the properties of the electrodes. The error in (3.38) is of order M^{-1} or $(lM^{\frac{1}{2}})^{-3}$, whichever is the larger.

The comparison between the theoretical prediction of R/R_∞ and the experimental values is displayed in figure 3 and is discussed further in § 5.

the equation becomes

$$(m_1'+n_1')[(a-1)+(3-2a)|m_2'|^2]+(m_2'+n_2')[(a-1)+|m_1'|^2+(2-a)|m_2'|^2]+a[m_1'm_2'^2+n_1'n_2'^2]=0. \quad (3.15)$$

All the terms occurring in (3.15) are real and, if we write

$$m_1' = r_1 e^{i\gamma_1}, \quad m_2' = r_2 e^{i\gamma_2},$$

then (3.15) becomes

$$r_1\cos\gamma_1[(a-1)+(3-2a)r_2^2]+r_2\cos\gamma_2[(a-1)+r_1^2+(2-a)r_2^2]+ar_1r_2\cos(\gamma_1+2\gamma_2). \quad (3.16)$$

Solving for r_1, r_2, γ_1 and γ_2 in terms of δ and T and then substituting in (3.16) gives the equation

$$5+T+(T-3)\sqrt{q}+\left(\frac{\sqrt{q}+1}{\sqrt{p}+1}\right)^{\frac{1}{2}}\{2+(T+1)\sqrt{p}+(r-1)\sqrt{q}\}+(T+1)(T+3)\frac{\delta}{2}\left(\frac{\sqrt{p}-1}{\sqrt{p}+1}\right)^{\frac{1}{2}}=0, \quad (3.17)$$

where

$$p = 1+\left(\frac{T-1}{2}\right)^2\delta^2, \quad q = 1+\left(\frac{T+1}{2}\right)^2\delta^2. \quad (3.18)$$

We immediately note from (3.17) that, if $T \geqslant 3$, then, since all the terms are positive, there can be no real values of δ satisfying the equation. This means that $c = 0$ is not an eigenvalue if $T > T_{\text{crit}}$, where

$$1 < T_{\text{crit}} < 3. \quad (3.19)$$

Equation (3.17) was solved numerically and gave

$$T_{\text{crit}} \doteqdot 1{\cdot}0456. \quad (3.20)$$

Next we show that the left-hand side of (3.17) has a different behaviour in the case $T = 1$ (i.e. zero magnetic field) as compared with the case $T > 1$.

Let us write (3.17) as $F(\delta, T) = 0$. Then, when $T = 1$

$$F(\delta,1) = 6+2\sqrt{2}(1+\sqrt{(1+\delta^2)})^{\frac{1}{2}}-2\sqrt{(1+\delta^2)}. \quad (3.21)$$

For large values of δ $\quad F(\delta,1) \sim 2\sqrt{2}\,\delta^{\frac{1}{2}}-2\delta,$

and is seen to be negative. When $\delta = 0$, F has the value 8, so that the equation $F(\delta,1) = 0$ is deemed to have an odd number of real positive roots. In fact there is only one root $\delta = 4\sqrt{3}$ as is easily found from (3.21) by squaring twice to eliminate radicals. This is as found by Esch (1957), Tatsumi & Gotoh (1960) and Drazin (1961).

On the other hand, when $T > 1$, then for large values of δ

$$F(\delta,T) \sim (T+1)\{T+(T^2-1)^{\frac{1}{2}}\}\delta,$$

and is seen to be positive. When $\delta = 0$, F has the value $4(T+1)$ which is also positive, so that if real positive roots exist they must be even in number.

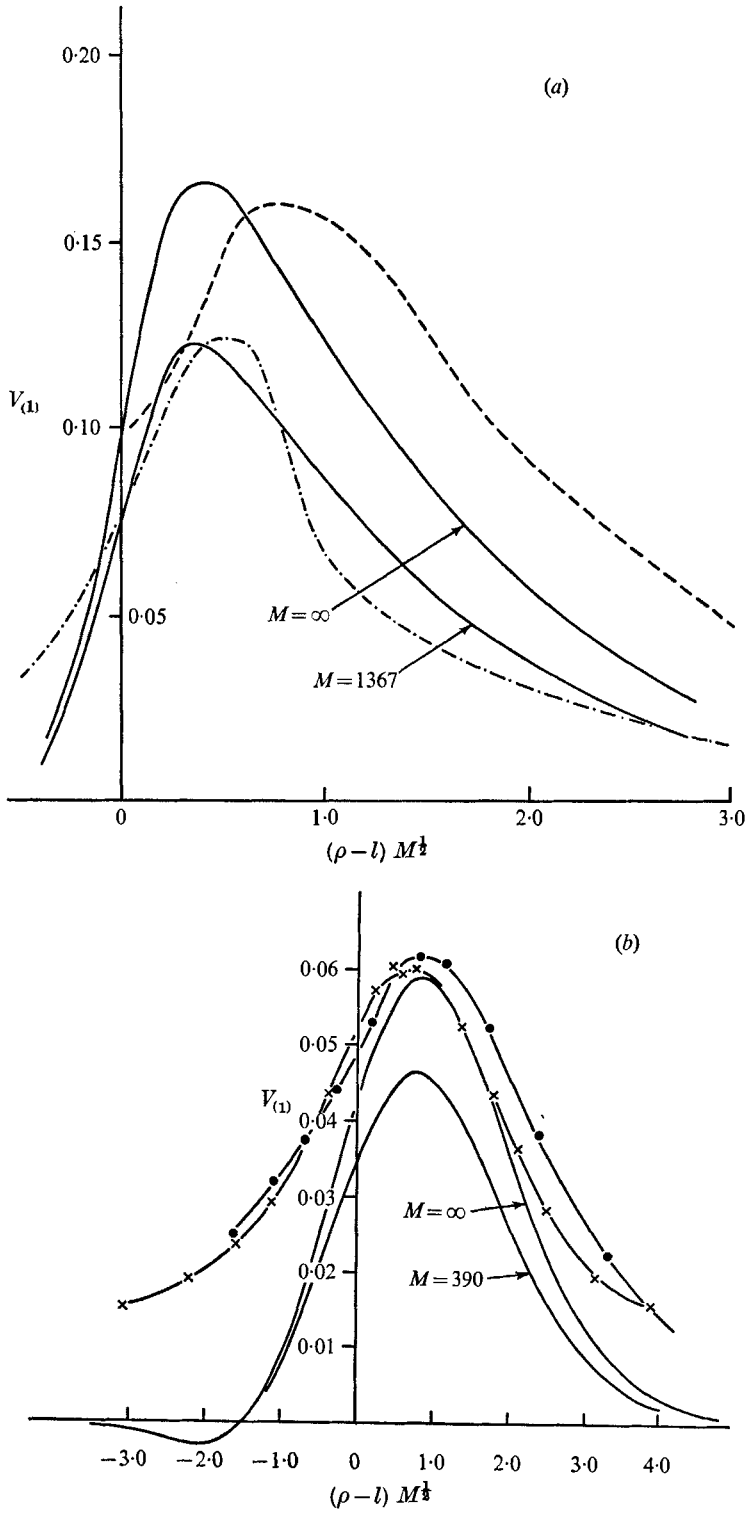

FIGURE 4. $V_{(1)} = v_\theta M^{\frac{1}{2}} l^2 a \sqrt{(\sigma\eta)}/I$ against $(\rho-l)\,M^{\frac{1}{2}}$. (*a*) $M = 1367$, $\zeta = 0{\cdot}97$, $\zeta = 0{\cdot}190$. ——, theoretical curves (zero-order and first-order). Experimental curves: – – –, results from Pitot tube; —·—, results from potential probe. (*b*) $M = 212, 390$, $\zeta = 0{\cdot}50, l = 0{\cdot}502$. ——, theoretical curves (zero-order and first-order). Malcolm's experimental curves: ×——×, $M = 390$; •—•, $M = 212$.

graphs of $V_{(1)}$ against $(\rho-l)M^{\frac{1}{2}} = -2\hat{\rho}$, taking the values of l, M and ζ used by Hunt & Malcolm, and by Malcolm, these being, in figure 4(*a*),

$$\zeta = 0{\cdot}97, \quad M = 1367, \quad l = 0{\cdot}190,$$

and in figure 4(*b*) $\quad \zeta = 0{\cdot}50, \quad M = 390, \quad l = 0{\cdot}502.$

From these curves we note how rapidly the velocity rises near $\zeta = 1$, a consequence of the result that in region (2) $v = 0$ for $\rho < l$ or, in physical terms, the fact that no Hartmann boundary layer can form on the electrodes; at $\zeta = 0{\cdot}50$, it is interesting to observe that a small negative velocity is predicted by the theory. The experimental results are discussed in § 5.

To calculate Φ we use (2.3) and the fact that in region (1) $\partial h/\partial\zeta$ is $O(M^{-1})$ compared with $\partial\Phi/\partial\rho$ and Mv. Then

$$\frac{\partial\Phi}{\partial\rho} = Mv = M(l/\rho)^{\frac{1}{2}}\hat{v},$$

so that

$$\Phi_{(1)} = -M\int_{-\infty}^{\hat{\rho}} \frac{2l\hat{v}(t)\,dt}{lM^{\frac{1}{2}} - 2t}.$$

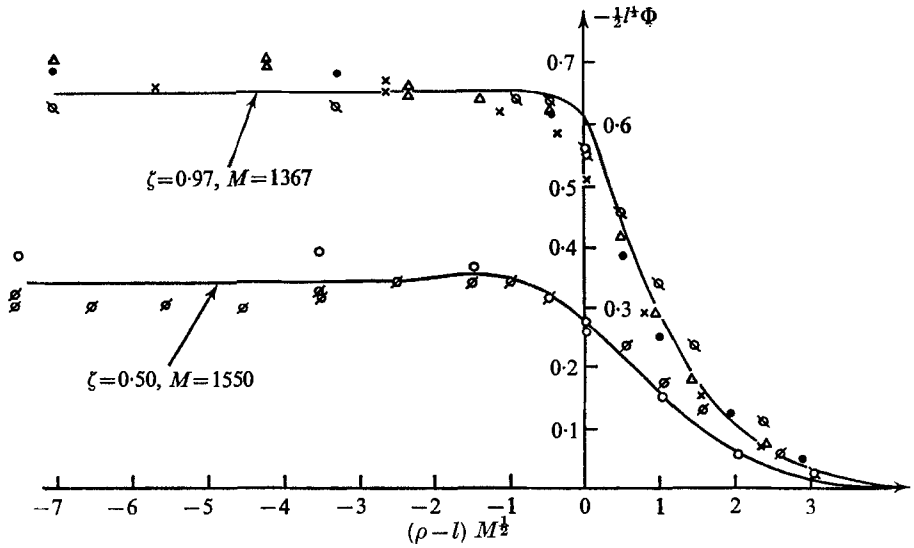

FIGURE 5. $-\frac{1}{2}l^{\frac{1}{2}}\Phi$ against $(\rho-l)\,M^{\frac{1}{2}}$ for $l = 0{\cdot}190$. ——, theoretical curves (first-order only). Experimental points: △, $M = 1367$, $\zeta = 0{\cdot}97$; ×, $M = 882$, $\zeta = 0{\cdot}99$; ●, $M = 1367$, $\zeta = 0{\cdot}99$; ⊘, $M = 1367$, $\zeta = 0{\cdot}96$; ○, $M = 1550$, $\zeta = 0{\cdot}50$; ⌀, $M = 1575$, $\zeta = 0{\cdot}50$.

Then, neglecting terms of $O(M^{-1})$ and $O[(lM^{\frac{1}{2}})^{-3}]$,

$$\Phi_{(1)} = \frac{4}{l^2\sqrt{\pi}}\left\{K(\hat{\rho},\zeta) + \frac{1}{lM^{\frac{1}{2}}}\left[\left(\frac{3\lambda_{\mathrm{I}}}{4}+\hat{\rho}\right)K(\hat{\rho},\zeta) - \int_{-\infty}^{\hat{\rho}} K(t,\zeta)\,dt\right]\right\}, \tag{3.40}$$

where

$$K(\hat{\rho},\zeta) = \int_{-\infty}^{\hat{\rho}}\left\{\int_0^{\infty} g(t_1)\left[\frac{e^{-(t_1-t)^2/(1-\zeta)}}{\sqrt{(1-\zeta)}} - \frac{e^{-(t_1-t)^2/(1+\zeta)}}{\sqrt{(1+\zeta)}}\right]dt_1\right\}dt.$$

To compute $\Phi_{(1)}$ from (3.40) we had to compute $V_{(1)}$ twice, a process possibly leading to some error. However, we found in our results that, when $M = \infty$,

$-\frac{1}{2}l^2\Phi_{(1)} = 0{\cdot}9725$ when $\hat{\rho} = 3$ and $\zeta = 0{\cdot}97$, and $0{\cdot}4999$ when $\hat{\rho} = 3$ and $\zeta = 0{\cdot}50$, whereas the correct values for $-\frac{1}{2}l^2\Phi_{(1)}$ to match with in region (4) should have been $0{\cdot}970$ and $0{\cdot}50$, respectively. This indicates that the computations may be relied upon to within 1 %.

In figure 5 we present graphs of our theoretical values of $-\frac{1}{2}l^2\Phi_{(1)}$ against $(\rho - l)M^{\frac{1}{2}}$ for the following values of ζ and M, with $l = 0{\cdot}190$:

$$\zeta = 0{\cdot}97, \quad M = 1367,$$

$$\zeta = 0{\cdot}50, \quad M = 1550.$$

These results, which are plotted together with the experimental values found by Hunt & Malcolm, are compared in § 5.

4. The form of the solution near the edge of an electrode, region (3)

The discussion in the previous section has shown that the discontinuity in h at $\rho = l$, as implied by the solutions in regions (4) and (5), is smoothed out by a shear layer, region (1), of thickness $O(M^{-\frac{1}{2}})$, except at $\zeta = \pm 1$. Here, although the shear layer extends to the electrodes it only succeeds in reducing the discontinuity in h from $-4\zeta(\frac{1}{2})/l^2\sqrt{(2\pi M)}$ to $2\sqrt{2}/l^2M^{\frac{1}{2}}$, from (3.34) and (3.35), where terms $O(M^{-1}l^2)$ have been neglected. The physical interpretation of this surprising result is that a weak ring source of current, of strength $2I\sqrt{2}/lM^{\frac{1}{2}}$, is set up on one electrode at $\rho = l$ and a corresponding sink at the other. Nevertheless the current density must become large as $M \to \infty$ because the thickness of the ring source is $o(M^{-\frac{1}{2}})$ and in fact, as we shall see, $O(M^{-1})$. The aim in this section is to analyze the structure of the ring source at $\zeta = 1$. For this purpose we make the following change of variables:

$$x = \tfrac{1}{2}M(\rho - l), \quad y = \tfrac{1}{2}M(1-\zeta),$$

$$H(x,y) = \frac{l^2M^{\frac{1}{2}}}{2\sqrt{2}}\left(\frac{1}{l} - h\right), \quad V(x,y) = -\frac{l^2M^{\frac{1}{2}}}{2\sqrt{2}}v, \tag{4.1}$$

and take the limit $M \to \infty$, keeping x, y, H, V finite. The net result is that the curvature of the electrode at $\zeta = 1$ and the effect of the other electrode at $\zeta = -1$ may both be neglected.

The governing equations for V and H reduce therefore to

$$\frac{\partial^2 V}{\partial x^2} + \frac{\partial^2 V}{\partial y^2} - 2\frac{\partial H}{\partial y} = 0, \quad \frac{\partial^2 H}{\partial x^2} + \frac{\partial^2 H}{\partial y^2} - 2\frac{\partial V}{\partial y} = 0, \tag{4.2}$$

with boundary conditions

$$V = 0, \quad H = 0, \quad \text{if} \quad x < 0 \quad \text{and} \quad V = 0, \quad \frac{\partial H}{\partial y} = 0 \quad \text{if} \quad x > 0, \tag{4.3}$$

at $y = 0$.

When $y > 0$ the conditions on V, H as $x \to \pm\infty$ demand some care. First we note that the solution for $\hat{v} + \hat{h}$ cannot have a boundary layer near $\zeta = 1$ and so

$$V + H \to 1 \quad \text{as} \quad x \to -\infty, \quad V + H \to 0 \quad \text{as} \quad x \to +\infty, \tag{4.4}$$

for $y > 0$, to match with (3.23). On the other hand $-\hat{v}+\hat{h}$ can have a boundary layer near $\zeta = 1$ and so to match with the analogue of (3.24), (3.25), (3.26), (3.27)

$$H - V \to 1 \quad \text{as} \quad x \to -\infty, \quad H - V \to 1 - e^{-2y} \quad \text{as} \quad x \to +\infty. \tag{4.5}$$

The reader is reminded that a primary boundary layer cannot occur in the neighbourhood of the electrodes.

In order to solve (4.2) subject to these boundary conditions we define

$$H(x, 0) = m(x) \quad \text{and} \quad \left.\frac{\partial H}{\partial y}\right|_{y=0} = n(x). \tag{4.6}$$

Next we take the Fourier transforms of $V, H, m(x), n(x)$ with respect to x, denoting the results by bars. Thus

$$\overline{V}(\omega; y) = \int_{-\infty}^{\infty} e^{-i\omega x} V(x, y)\, dx, \quad V(x, y) = \frac{1}{2\pi}\int_{-\infty}^{\infty} e^{i\omega x}\overline{V}(\omega; y)\, d\omega. \tag{4.7}$$

Then, adding the two equations of (4.2) and using (4.5),

$$\overline{V} + \overline{H} = \overline{m}\, e^{y(1-p)}, \quad \text{where} \quad p = (\omega^2 + 1)^{\frac{1}{2}}, \tag{4.8}$$

p being real and positive when ω is real. Similarly

$$\overline{H} - \overline{V} = \overline{m}\, e^{-y(1+p)}. \tag{4.9}$$

Hence, subtracting (4.9) from (4.8) and differentiating with respect to y,

$$2\overline{n} = -2p\overline{m}. \tag{4.10}$$

Here $\overline{m}$ is regular in the upper half plane $\operatorname{Im}\omega > 0$ since $m(x) = 0$ when $x > 0$ and $\overline{n}$ is regular in the lower half plane $\operatorname{Im}\omega < 0$ since $n(x) = 0$ if $x < 0$. Now consider

$$\overline{m}_1 = -\frac{e^{-\frac{1}{4}i\pi}}{(\omega - i\epsilon)(\omega + i)^{\frac{1}{2}}} \quad (\epsilon > 0), \tag{4.11}$$

whose inverse transform is

$$-\frac{1}{\pi}\int_1^{\infty} \frac{e^{tx}\, dt}{(t+\epsilon)(t-1)^{\frac{1}{2}}} \quad \text{if} \quad x < 0 \quad \text{and} \quad -\frac{e^{-\epsilon x}}{(1+\epsilon)^{\frac{1}{2}}} \quad \text{if} \quad x > 0,$$

reducing to

$$-\frac{1}{\sqrt{\pi}}\int_{-x}^{\infty} \frac{e^{-s}\, ds}{s^{\frac{1}{2}}} \quad \text{if} \quad x < 0 \quad \text{and} \quad -1 \quad \text{if} \quad x > 0 \tag{4.12}$$

in the limit $\epsilon \to 0$. From (4.9) the corresponding value of $\overline{n}$ is

$$\overline{n}_1 = \frac{e^{-\frac{1}{4}i\pi}(\omega - i)^{\frac{1}{2}}}{(\omega - i\epsilon)},$$

whose inverse transform clearly vanishes when $x < 0$ as required by (4.5). The only condition which $\overline{m}_1, \overline{n}_1$ fail to satisfy therefore is that $\overline{m}_1(x) \neq 0$ if $x > 0$ and this may easily be rectified by adding unity to the corresponding value of H. The final solution for H is then

$$H = 1 - \frac{\cosh y}{2\pi}\int_{-\infty}^{\infty} d\omega\, \frac{\exp\{i\omega x - \frac{1}{4}i\pi - y(\omega^2+1)^{\frac{1}{2}}\}}{\omega(\omega + i)^{\frac{1}{2}}}, \tag{4.13}$$

where the path of integration passes *below* the origin of ω. It may readily be verified that (4.13) satisfies all the required boundary conditions and we have

$$H(x,0) = \frac{1}{\sqrt{\pi}}\int_0^{-x} \frac{e^{-s}\,ds}{s^{\frac{1}{2}}}$$

when $x < 0$, which tends to unity as $x \to -\infty$ and behaves like $2(-x)^{\frac{1}{2}}/\sqrt{\pi}$ as $-x \to 0$. Thus $H(x,0)$ is continuous at $x = 0$ with its null value when $x > 0$. Further, the singularity at $x = 0-$ has the same structure as when $M = 0$, and indeed, in terms of $l-\rho$, is independent of M. Finally,

$$n(x) \equiv \left.\frac{\partial H}{\partial y}\right|_{y=0} = \frac{1}{\sqrt{\pi}}\int_0^{x} \frac{e^{-s}\,ds}{\sqrt{s}} + \frac{e^{-x}}{\sqrt{(\pi x)}}$$

when $x > 0$; near $x = 0$, $n(x) \approx (\pi x)^{-\frac{1}{2}}$, and $n(x) \to 1+$ as $x \to \infty$.

5. Discussion

In the experiments of Hunt & Malcolm (1968), distributions of electric potential and velocity were measured in mercury held in a plastic container between copper electrodes. In the apparatus two different values of l, the ratio of the diameter of the electrodes to the distance between them, were obtained, 0·512 and 0·190 respectively. The relative resistance of the electrodes to the fluid defined by $\sigma a/\sigma_e t$ was 0·049 and 0·130 respectively, so that we can regard the electrodes as being highly conducting.

In order that the experimental results when $M > 0$ should be credible, measurements were made of the resistance R when $M = 0$, and then compared with the theoretical value. This measurement could only be made for the first apparatus in which $l = 0{\cdot}512$, $b = 8{\cdot}25$ mm, $\sigma = 1{\cdot}04 \times 10^6$ mho/m, giving

$$R = 40{\cdot}7 \times 10^{-6} \pm 0{\cdot}5 \times 10^{-6} \text{ ohms}. \tag{5.1}$$

To calculate the theoretical value, the equation (2.2) with $M = 0$, namely

$$\frac{\partial^2 h}{\partial \rho^2} + \frac{1}{\rho}\frac{\partial h}{\partial \rho} - \frac{h}{\rho^2} + \frac{\partial^2 h}{\partial \zeta^2} = 0, \tag{5.2}$$

has to be solved subject to the boundary conditions (2.9) and (2.11). This problem is equivalent to finding the capacity of a disk at a potential $\Delta\phi$ placed between two plates at zero potential, and, as such, has been extensively studied in the past (Tranter 1950, Collins 1960). The resistance, R_0, is found to be

$$R_0 = \frac{1}{2b\sigma}\left[1 - \frac{2\log 2}{\pi}l + \frac{\zeta(3)\,l^3}{4\pi} + \ldots\right], \tag{5.3}$$

which, using the experimental values, gives

$$R_0 = 39{\cdot}6 \times 10^{-6} \text{ ohms}. \tag{5.4}$$

The discrepancy between the experimental (5.1) and the theoretical results (5.4) may be caused by the fact that the walls containing the fluid tend to confine the current lines and so raise the value of R.

The main purpose of the experiments was to confirm the interesting phenomena which occur when $M \gg 1$ as predicted by the approximate analysis of Hunt & Malcolm. Since then we have developed the asymptotic theory described in §§ 3–4 and we now compare the results. The experimental results least subject to error are those we ought to refer to first in assessing the experiments in the light of the theory, and therefore we consider the results in figure 3, namely the ratio R/R_∞ against $1/lM^{\frac{1}{2}}$. We see that the agreement between the theoretical line and the experiment is remarkable (at least by the standards of magneto-hydrodynamics experiments), any systematic discrepancy being under 3 %.

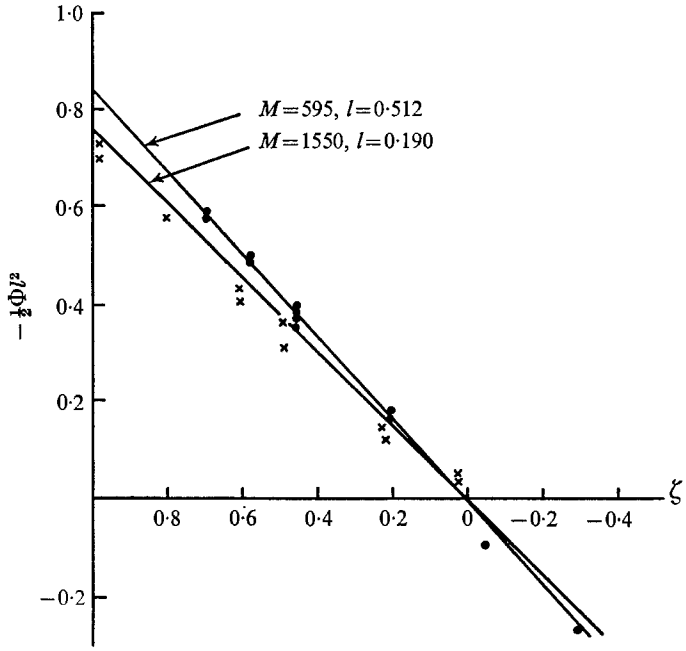

FIGURE 6. $-\frac{1}{2}l^2\Phi$ against ζ on the line $\rho = 0$. ——, theoretical curves (which include first-order and second-order terms). ●, $l = 0{\cdot}512$; ×, $l = 0{\cdot}190$.

We note than the higher-order terms ignored in (3.38) would produce a change of under 1 % at $(lM^{\frac{1}{2}})^{-1} = 0{\cdot}18$. In figure 6 the values of $\frac{1}{2}l^2\Phi$ on the line $\rho = 0$ are plotted for $l = 0{\cdot}512$ and $l = 0{\cdot}190$. These are the most reliable probe measurements because, since most probe errors are caused by the change in the velocity produced by the probe, the velocity is zero in region (4). The theoretical curves also displayed in figure 6 have been calculated from (3.37) using the values of λ_1 and λ_2 in (3.33), so that these theoretical curves include the second-order terms. The agreement between the theory and the experiments is most satisfactory for the highest value of $1/(lM^{\frac{1}{2}})$, where there is no discernible systematic error. On the other hand for $l = 0{\cdot}190$, where $1/lM^{\frac{1}{2}} = 0{\cdot}134$, the experimental points fall systematically below the theoretical line, a discrepancy we also find in the results of figure 3. However, considering the experimental scatter and the relatively few number of points, the small difference between the theory and experiment in this case is not, we believe, significant.

In figure 4(*a*) we have plotted the theoretical values of $V_{(1)} = v_\theta l^2 Ma \sqrt{(\sigma\eta)}/I$ against $(\rho - l) M^{\frac{1}{2}}$, on the same graph as the experimental values. These two experimental curves were obtained in the one case by using a Pitot tube to measure v_θ directly, and in the other by measuring ϕ and then calculating v_θ from the relation, used in § 3,

$$0 = -\frac{\partial \phi}{\partial r} + B_0 v_\theta,$$

so that

$$V_{(1)} = \frac{\partial \phi}{\partial r} \sigma l^2 a^2 M^{-\frac{1}{2}}/I.$$

As explained by Hunt & Malcolm, both these different methods have considerable errors and it is therefore of great interest, in assessing the respective reliabilities of these methods, that the theoretical curve which includes the first-order correction falls very much closer to the curve calculated from potential probe measurements than from the Pitot-tube measurements. This result should not be regarded as a final verdict on the relative merits of these two probes for two reasons: first, the agreement with the results of the potential probe may be somewhat fortuitous because, in calculating these results, a crudely estimated error term had to be used; secondly, the Pitot tube was being used in a region of large variations in static pressure which also had to be estimated. (The details of these calculations are given by Hunt & Malcolm (1968).) However, this result and those discussed later do indicate that electric potential probes can give reasonably accurate results.

In figure 4(*b*) we have plotted Malcolm's results and we find that the experimental velocity profiles follow that calculated from the zero-order theory quite closely over a limited range of ρ ($-1{\cdot}0 > (\rho - l) M^{\frac{1}{2}} > 3{\cdot}0$). However, although the experimental velocity profile has the same shape as that of the first-order theory, the experimental results are greater by an amount 20 % or more of the maximum velocity of the theoretical profile. Further, the value of $V_{(1)}$ is greater for $M = 212$ than 390, whereas the theory predicts the reverse. Malcolm (1968) suggests that these discrepancies are caused by the magnetic field affecting the heat transfer characteristics of the hot-film anemometer. These errors may be further increased because the anemometer, as well as recording the azimuthal velocity, is also sensitive to a radial velocity which is produced by the small secondary flow. For further details of this problem and the transition to an oscillatory secondary flow the reader is referred to Malcolm (1968).

In figure 5 we have compared the experimental and theoretical values of $-\frac{1}{2} l^2 \Phi = -\Phi \sigma \pi b^2/Ia$ as a function of $(\rho - l) M^{\frac{1}{2}}$ at $\zeta = 0{\cdot}97$, and $\zeta = 0{\cdot}50$ for $l = 0{\cdot}190$. We find that for $\zeta = 0{\cdot}97$ there is a small, systematic discrepancy between our theory and the experimental results, greater than that attributable to random errors, for $-1 > (\rho - l) M^{\frac{1}{2}} > 0{\cdot}25$, in much the same way as with the velocity at $\zeta = 0{\cdot}97$. These discrepancies occur where $|\partial^2 \Phi/\partial \rho^2|$ is greatest and therefore where the effects of the finite size of the probe are most significant, as shown by Hunt & Malcolm. We have not allowed for this error so that the discrepancy may be seen. However, this probe error was estimated in calculating v_θ from the measured values of ϕ in figure 4(*a*), as referred to above. It is also

possible that some of the discrepancies, near $\rho = l$ and $\zeta = 1$, between our theory and the experiments are a result of the finite conductivity of the electrode, which our theory does not allow for. When $\zeta = 0{\cdot}50$ and the gradients are more gentle, we find satisfactory agreement between the theoretical and experimental values.

Our main conclusions, then, are these. (i) Those measurements of which we feel most confident, namely the resistance between the electrodes and the potential distribution on $\rho = 0$, differ from the theoretical values by less than the experimental error. These provide, therefore, further evidence of the validity of the general theory of magneto-fluid-dynamic duct flows, of which §3 is an example. (ii) It is a characteristic of MHD flows with strong magnetic fields that the most interesting phenomena occur in narrow regions parallel to the magnetic field and this flow is no exception. Although the flow in these regions is the most difficult to measure, the experimental results in region (1) for electric potential (and velocity, when calculated from potential measurements) have shown good agreement with the theory; at least where the changes in potential gradient occur over distances small compared with the probe size. The experiments of Hunt & Malcolm (1968) were among the first measurements of such a region with flow conditions such that confirmation of the theoretical velocity and electric potential profiles is possible. (iii) As to the merits of the three kinds of probe referred to here, namely the Pitot tube, the electric potential probe and the hot-film anemometer, we conclude that the electric potential probe is probably the most reliable instrument, both for measuring potential and for calculating the velocity, when a simple relation exists between the electric potential and the velocity. In many flows such a relation does not exist, and in that case for measuring velocity the hot-film anemometer used by Malcolm (1968) is probably more satisfactory than the Pitot tube.

While the early part of work described in this paper was being carried out one of us (K.S.) benefited from the hospitality kindly provided by Prof. G. L. Von Eschen of Ohio State University. During the same period the other (J.C.R.H.) was being supported by the U.S. Army Research Office and he gratefully acknowledges the hospitality provided by Prof. G. S. S. Ludford of Cornell University. Finally, we should like to thank Dr D. G. Malcolm for making available his experimental results in advance of publication.

REFERENCES

COLLINS, W. D. 1960 *Proc. Edin. Maths. Soc.* (2nd series) **12**, 95.

GREEN, A. E. & ZERNA, W. 1960 *Theoretical Elasticity*, pp. 172–177.

HAMMERSLEY, J. M. 1961 *4th Berkeley Symposium on Mathematical Statistics and Probability*, vol. III. University of California Press.

HUNT, J. C. R. & MALCOLM, D. G. 1968 *J. Fluid Mech.* **33**, 775.

HUNT, J. C. R. & WILLIAMS, W. E. 1968 *J. Fluid Mech.* **31**, 705.

MALCOLM, D. G. 1968 *Proc. 6th Symposium on Magnetohydrodynamics*. Riga. To be published by Institute of Physics, Latvian Acad. of Sci., Riga, Latvia, in *Magnetohydrodynamics*.

STEWARTSON, K. 1968 *Mathematika*, **15**, 22.

TRANTER, C. J. 1950 *Q. J. Mech. Appl. Math.* **3**.